LWT - Food Science and Technology 59 (2014) 641–648

Contents lists available at ScienceDirect

LWT - Food Science and Technology

journal homepage: www.elsevier.com/locate/lwt

Corn starch-calcium alginate matrices for the simultaneous carrying of zinc and yerba mate antioxidants

Alex López-Córdoba, Lorena Deladino*, Miriam Martino

CIDCA, Centro de Investigación y Desarrollo en Criotecnología de los Alimentos, CONICET, Fac. Cs. Exactas (UNLP), 47 y 116, La Plata 1900, Argentina

ARTICLE INFO

Article history:
Received 14 March 2014
Received in revised form
3 June 2014
Accepted 9 June 2014
Available online 16 June 2014

Keywords:
Zinc
Yerba mate
Encapsulation
Calcium alginate
Natural antioxidant

ABSTRACT

A new strategy for the simultaneous carrying of zinc and yerba mate antioxidants into starch-alginate matrices was developed. Firstly, the use of native corn starch as vehicle of zinc was evaluated and then the starch-zinc carriers were incorporated into calcium alginate beads containing antioxidant extract of yerba mate. The loading capacity and the antioxidant activity of the beads were determined. Moreover, the systems were characterized by scanning electron microscopy (SEM), Fourier transform infrared spectrometry (FT-IR) and differential scanning calorimetry (DSC). Compartmentalized beads containing yerba mate polyphenols and zinc were obtained without affecting their morphological aspect. Moreover, the encapsulating systems exhibited a high antioxidant activity assayed by both, β-carotene linoleate model system and DPPH radical scavenging method. FT-IR and DSC analysis revealed that interactions between the active compounds and the encapsulating matrix were not formed. The proposed methodology constituted a useful strategy for the simultaneous transport of yerba mate antioxidants and zinc by preventing a possible interaction between them. The new beads could be incorporated into food formulations for preserving substances prone to oxidation and for providing compounds with beneficial properties for health.

1. Introduction

The production of foods that promotes health benefits beyond providing the nutritional and energetic requirements constitutes a challenge for the food industry. Therefore, there is an increasing interest on the development of functional ingredients. Many studies have focused on the role of reactive oxygen species in numerous diseases and have suggested the protective effect of antioxidant compounds (Brewer, 2011; Prasad, Bao, Beck, Kucuk, & Sarkar, 2004). Moreover, several authors reported the advantage of using a combination of antioxidant and minerals since these compounds could act not only individually but also cooperatively or synergistically (Hercberg et al., 2004; Yang et al., 2014). On this regard, the design of biopolymeric matrices for the simultaneous carrying of minerals and natural antioxidants constitutes a new approach for improving the functionality of the conventional encapsulation systems. This strategy would also help reducing the number of food additives. According to World Health Organization (WHO) the zinc is the most ubiquitous of all trace elements involved in human metabolism and its deficiency is a world nutritional problem. So, zinc requirements for dietary intake were recently adjusted upward for populations in which animal products, the best sources of zinc, are limited, and in which plant sources of zinc are high in absorption inhibitors such as phytates (WHO, 2002). Zinc plays important roles in immune system control, wound healing, growth control, and acts as a cofactor for various metalloenzymes (Salgueiro et al., 2000; Tapiero & Tew, 2003). Additionally, Zn^{2+} has shown to have an antioxidant role in defined chemical systems (Goel, Dani, & Dhawan, 2005; Zago & Oteiza, 2001). Zinc sulfate, listed as generally regarded as safe (GRAS), is one of the most commonly used Zn compounds for food fortification. This salt has the advantage of being low cost and bioavailable (Salgueiro et al., 2000). Yerba mate (*Ilex paraguariensis*) extract constituted an important source of bioactive compounds including polyphenols, xanthines, flavonoids, saponins, amino acids, minerals and vitamins (Heck & González de Mejía, 2007). Several studies have demonstrated that this extract has antioxidant, hepatoprotective, choleretic, diuretic, hypocholesterolemic, antirheumatic, antithrombotic, antiinflammatory, antiobesity and antiageing properties (Bracesco, Sanchez, Contreras, Menini, & Gugliucci, 2011).

* Corresponding author. Tel./fax: +54 92214254853.
E-mail address: loredeladino@gmail.com (L. Deladino).

http://dx.doi.org/10.1016/j.lwt.2014.06.021
0023-6438/

Both zinc and yerba mate extract are chemically reactive and their functionality could be affected by interactions with other components of the food matrix. In addition, depending of the concentration used, they may modify sensory characteristics of foods. In this sense, encapsulation constituted a way to protect bioactive compounds against adverse conditions and mask unpleasant flavors (Day, Seymour, Pitts, Konczak, & Lundin, 2009). Calcium alginate beads can be formed by dropping a sodium alginate solution into a bath of divalent or polyvalent cations. This method has the advantage to be simple, fast and environmental friendliness (George & Abraham, 2006). However, some disadvantages for calcium alginate beads have been reported; for example it is well known that these have high porosity and poor mechanical properties (Fundueanu, Nastruzzi, Carpov, Desbrieres, & Rinaudo, 1999; Rassis, Saguy, & Nussinovitch, 2002). One of the methods used currently to improve the characteristics of alginate gels is the incorporation of a filler material into the matrix. For this purpose, corn starch has been used in previous works demonstrating that the incorporation of starch as filler into the alginate matrix lead to higher encapsulation efficiencies and a delayed release rate of yerba mate polyphenols in simulated digestive fluids. Additionally, the porosity of the matrices diminished and their original shape was maintained after drying (López Córdoba, Deladino, & Martino, 2013, 2014).

Another disadvantage for alginate beads is the encapsulation of transition metals (e.g. Zn^{+2}, Fe^{+2}) or transition metals-rich compounds (e.g. some herbal extracts). Some metals could crosslink alginate chains competing with Ca^{2+} and consequently larger capsules, with ununiformed size and irregular shape were reported (Belščak-Cvitanović et al., 2011). To face this drawback we developed a completely new strategy to achieve the simultaneous carrying of yerba mate antioxidants and zinc within a starch-alginate matrix. The objectives of this work were (i) to evaluate whether a compartmentalized system for the simultaneous carrying of yerba mate polyphenols and zinc sulfate, could be obtained employing a calcium alginate matrix filled with native corn starch; (ii) to analyze possible interactions between the active compounds; and (iii) to characterize the microstructure of the combined system.

2. Materials and methods

2.1. Materials

The encapsulating materials employed were corn starch (Molinos Río de la Plata, Argentina) and sodium alginate (Sigma-Aldrich, USA). Active compounds were zinc sulfate (Anedra, Argentina) and a natural extract of yerba mate (Las Marías, Corrientes, Argentina). Other reagents were chlorogenic acid (Fluka, USA), Folin-ciocalteu reagent (Anedra, Argentina); sodium bicarbonate (Anedra, Argentina); 1,1-diphenyl-2-picrylhydrazyl (DPPH•) (Sigma–Aldrich, USA); Tween 40 (Sigma–Aldrich, Argentina) and β-carotene (Sigma–Aldrich, Argentina).

2.2. Preparation of aqueous extracts of yerba mate

The extracts were prepared according to the previously optimized methodology by Deladino, Anbinder, Navarro, and Martino (2008). Briefly, a blend of 3 g of commercial yerba mate and 100 mL of distillated water was placed in a thermostatic bath (Viking, Argentina) at 100 °C for 40 min. After this time, samples were filtered, cooled and kept in dark flasks until used.

2.3. Preparation of the biopolymeric matrices

The systems for simultaneous carrying of yerba mate extract and zinc were obtained in two stages (Fig. 1):

2.3.1. Stage 1: Preparation of the starch-zinc carriers

Blends of corn starch (1 g), deionized water (10 mL) and different amounts of zinc sulfate (1.3, 2.7 and 4 g/g of starch) were prepared under continuous stirring (180 rpm, 25 °C, 15 h). Then, the samples were centrifuged, the supernatant was removed and the

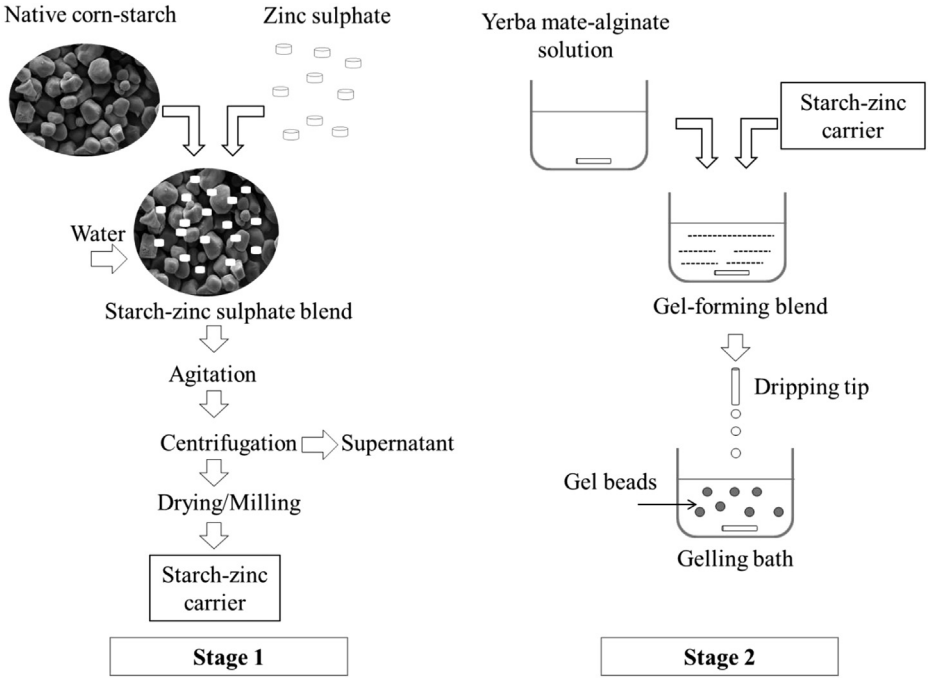

Fig. 1. Preparation process of corn starch-calcium alginate matrices with yerba mate extract and zinc.

solids were dried and milled. These products will be referred as "starch-zinc carriers".

2.3.2. Stage 2: Preparation of the beads with zinc and yerba mate extract

Corn starch-calcium alginate beads were prepared as described previously (López Córdoba et al., 2014). Briefly, a yerba mate extract-alginate solution was obtained dissolving 2 g of sodium alginate in 100 mL of extract. Then, 2 g of the starch-zinc carrier were added in this solution. Once homogenized and degassed by ultrasound, the solutions were forced with a peristaltic pump at 45 rpm (Gilson Minipuls 3, France) into a syringe (diameter: 1 mm) to drop into a calcium chloride solution (0.05 mol/L). The beads were maintained in the gelling bath to harden for 15 min and then filtered and washed with an acetic-acetate buffer solution at 0.02 mol/L (pH = 5.5). Finally, the beads were dried in a convection oven (SanJor, Argentina) at 65 °C until constant weight and maintained in a desiccator with silica gel. Dry weight of the beads was 0.05 g dried beads/g wet sample and the water activity was 0.5.

2.4. Determination of the zinc content

The zinc content was quantified by atomic absorption spectrophotometry using the flame method with a wavelength of 213.9 nm. The analyses were carried out in a Varian spectrometer model EspectrAA 300-plus (Cambridge, United Kingdom). Previously, the samples were digested with concentrated nitric acid.

2.5. Total polyphenols content

Total polyphenols content (TPC) was determined by the Folin-Ciocalteu method (Singleton, Orthofer, & Lamuela-Raventós, 1999). Briefly, 2 mL of Na_2CO_3 (2 g/100 mL) were mixed with 200 μL of the sample and 200 μL of Folin-Ciocalteu reagent (1:1 diluted). After 30 min, sample absorbance was measured at 725 nm in a spectrophotometer (Shimadzu, UV-mini 1240, Japan). Chlorogenic acid solutions of know concentration were used for calibration.

2.6. Loading capacity of the beads

The content of active compounds encapsulated was estimated by dissolving a known amount of beads in sodium citrate solution (5 g/100 mL) under agitation (Orbit Environ Shaker, Lab Instruments, USA) at 25 °C. The TPC was quantified by Folin-Ciocalteu method (Section 2.5) and the zinc content by atomic absorption spectrophotometry (Section 2.4). The loading capacity was calculated as the ratio between the active compound concentration in the citrate solution and the mass of dried beads employed in the assay.

2.7. Physicochemical characterization of the beads

2.7.1. Scanning electron microscopy (SEM)

SEM analysis was performed using a FEI, Quanta 200 microscope (Netherlands). Samples were attached to stubs using a two-sided adhesive tape, coated with a layer of gold (40–50 nm) and examined using an acceleration voltage of 20 kV. Cross sections were obtained by cryo-fracture immersing the capsules in liquid nitrogen. SEM-EDX analysis was performed using a ZEISS DSM-960 microscope equipped with an EDX (ISIS-LINK, Oxford Inst.) unit, to observe zinc sulfate distribution on starch granule surface. Samples were previously dispersed in a conductive coal band.

2.7.2. Size and morphological aspects

The maximum (d_{max}) and minimum (d_{min}) Feret's diameters were calculated analyzing the photographs of at least 100 beads with the ImageJ processing software (Schneider, Rasband, & Eliceiri, 2012). Feret's diameters are defined as the longest (d_{max}) and shortest (d_{min}) distance between any two points along the particle boundary.

The morphological parameters were calculated as follow:

$$E = \frac{d_{max}}{d_{min}} \quad (1)$$

$$SF = \frac{d_{max} - d_{min}}{d_{max} + d_{min}} \quad (2)$$

where E corresponds to elongation and SF to sphericity factor. E varies from unity for a perfect sphere to approaching infinity for an elongated particle whereas SF varies from 0 for a perfect sphere to approaching unity for an elongated particle (Chan, Lee, Ravindra, & Poncelet, 2009).

2.7.3. Antioxidant activity

A known amount of beads was disintegrated by crushing, blended with an appropriate volume of distilled water and placed on an orbital shaker for 20 h, at 180 rpm and room temperature. The antioxidant activity was assayed as follows:

2.7.3.1. DPPH• radical scavenging ability. The free radical scavenging activity towards the 1,1-diphenyl-2-picryl-hydrayl reagent (DPPH•) was determined according to the method described by Brand-Williams, Cuvelier, and Berset (1995). An aliquot of 100 μL of sample was mixed with 3.9 mL of DPPH• ethanol solution (25 mg DPPH•/L). Absorbance was determined at 517 nm until the reaction reached a plateau. The DPPH radical scavenging activity was expressed as the percentage of inhibition calculated as follows:

$$\text{DPPH}\cdot \text{ inhibition } (\%) = ((A_b - A_s)/A_b) \times 100 \quad (3)$$

where A_b is the absorbance of the blank and A_s is the absorbance of the sample.

2.7.3.2. β-carotene-linoleic acid assay. The β-carotene-linoleic acid assay was carried out as Valerga, Reta, and Lanari (2012). Firstly, 400 mg of Tween 40 and 40 mg of linoleic acid were weighted into a 100 mL round-bottomed flask. To this, 1 mL of β-carotene chloroform solution (3.34 mg/mL) was added. Next, chloroform was removed by evaporation at 40 °C under vacuum, the total volume was adjusted to 100 mL with distillated water (100 mL) and the blend was agitated vigorously to form an emulsion. A blank sample (without β-carotene) was prepared for background subtraction. Sample aliquots of 0.2 mL were blended with 5 mL of β-carotene-linoleic acid emulsion and the zero time absorbance at 470 nm was measured immediately. Then, the tubes were placed in a thermostatic bath at 40 °C for 120 min and the absorbance was measured again. The antioxidant activity was expressed as the inhibition percentage of the β-carotene bleaching calculated as follows:

$$\beta - \text{carotene bleaching inhibition}(\%) = (A_{t=120}/A_{t=0}) \times 100 \quad (4)$$

where $A_{t=0}$ is the absorbance of the reaction mixture at zero time and $A_{t=120}$ is the absorbance of the reaction mixture after 120 min at 40 °C.

2.7.4. Differential scanning calorimetry (DSC)

The equipment used was a DSC Q100 (TA Instruments, USA) calibrated with an Indium standard. Samples of 3–5 mg were placed in aluminum pans hermetically sealed and an empty pan was used as the reference. Samples were heated from 25 °C to 300 °C at a heating rate of 10 °C/min.

2.7.5. Fourier transform infrared spectrometry (FT-IR)

Disks (7 mm) were obtained by milling 1 mg of sample with 100 mg of KBr and were analyzed under transmission mode, taking 64 scans per experiment with a resolution of 4 cm^{-1}. The employed equipment was a Nicolet IS-10 (Thermo Scientific, USA) and the spectral analysis was performed with the software Omnic version 8.1 (Thermo Scientific, Inc., USA).

2.8. Statistical analysis

Data analysis was performed with the software SYSTAT INC. (Evanston, USA). Analysis of variance (ANOVA) and mean comparisons by Fisher Least Significant difference (LSD) test were carried out. Also, a *t*-test was performed. Unless indicated, a level of 95% of confidence ($\alpha = 0.05$) was used.

3. Results and discussion

3.1. Incorporation of the starch-zinc carriers into the alginate matrix

Starch-zinc carriers were obtained employing 0.32, 0.65 and 0.96 g of zinc (from zinc sulfate) per gram of starch (S-ZnL, S-ZnM and S-ZnH, respectively). Statistically significant differences were found in the zinc load ($p < 0.05$), with detected amounts of 16.5 ± 2.6 mg Zn/g starch for S-ZnL, 44 ± 6.4 mg Zn/g starch for S-ZnM and 64 ± 12.1 mg Zn/g starch in the case of S-ZnH. A similar behavior in the adsorption of zinc was observed by Smigielska and Thanh-Blicharz (2010) and Luo et al. (2013) working with potato and cassava modified starches, respectively.

When the starch-zinc carriers were incorporated into the alginate matrix significant changes in the morphology of the dried beads were observed compared with the control ones (Fig. 2). The S-ZnM and S-ZnH carriers gave gels of irregular shape and their drop-forming solutions were of difficult handling. According to Chan et al. (2009) the shape of liquid drop or bead could be classified into four basic types: spherical-shaped, tear-shaped, pear-shaped and egg-shaped. In the present work, before drying, the beads loaded with S-ZnL exhibited a spherical-shape as the control ones and after drying their sphericity was almost maintained (Fig. 2a and b). In contrast, the beads loaded with S-ZnM and S-ZnH showed a tear-shaped before and after drying (Fig. 2c). The morphology of the beads is a relevant factor from an industrial point of view. Several authors have reported that spherical beads have better handling properties, allowed maintaining the controlled release rate and also improving the visual aspect of the products in the case of food applications (Chan et al., 2009; Lesmes & McClements, 2009). For this reason, the characterization of the beads loaded with S-ZnM and S-ZnH carriers was not pursued further. The beads produced with S-ZnL and containing yerba mate antioxidants simultaneously will be referred as ZY-beads.

3.2. Characterization of the beads

3.2.1. SEM analysis

As can be observed in Fig. 3, starch filler was homogenously distributed in the inner core of the alginate matrix (Fig. 3b). Some starch granules were embedded into the surface, as well (Fig. 3a).

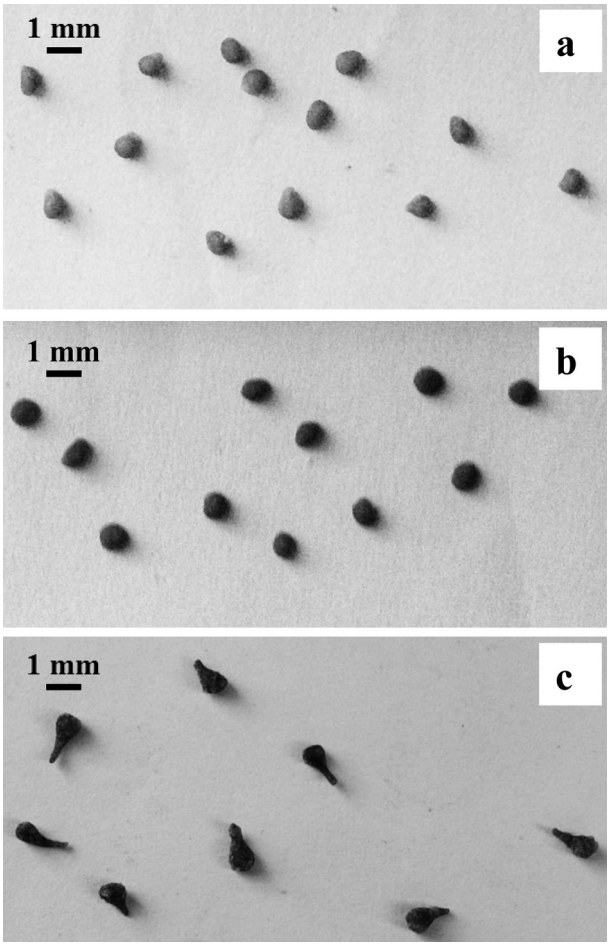

Fig. 2. Morphology aspect of (a) control beads, (b) SZnL-calcium alginate beads and (c) SZnM-calcium alginate beads. SZnL and SZnM: starch-zinc carrier with low and medium zinc concentration, respectively.

Energy dispersive X-ray microanalysis (EDX) was used to identify the location of mineral components on the starch granules. Micrographs confirmed a homogeneous distribution of both, zinc and sulfate on granule surface.

3.2.2. Size and morphological aspects

The particle size distribution and the shape parameters for control and ZY beads are shown in Fig. 4. The particle diameters ranged between 0.15 and 0.25 cm, nevertheless, differences between the size distribution profiles of the two types of beads were observed. ZY-beads showed a unimodal distribution with an average diameter of 0.18 ± 0.02 cm, whereas the control ones presented a bimodal distribution with an average diameter of 0.20 ± 0.03 cm (Fig. 4a). On the other hand, the zinc concentration used did not affect the values of sphericity and elongation (Fig. 4b and c) as compared with control beads. Previously, metal ions have been encapsulated by the conventional approach dissolving the metal into the alginate solution and, subsequently, extruding and cross-linking the resulting solution in a calcium bath. However, this preparation route promotes the interaction between the metal and the alginate, which results in a viscosity increase of the solution affecting the laminar liquid flow during extrusion and disrupting the formation of the beads (Chan, Jin, & Heng, 2002; Perez-Moral, Gonzalez, & Parker, 2013). Recently, Perez-Moral et al. (2013) proposed two strategies for achieving the encapsulation of Fe^{2+} and Fe^{3+} ions using an iron/calcium cross-linking bath or taking

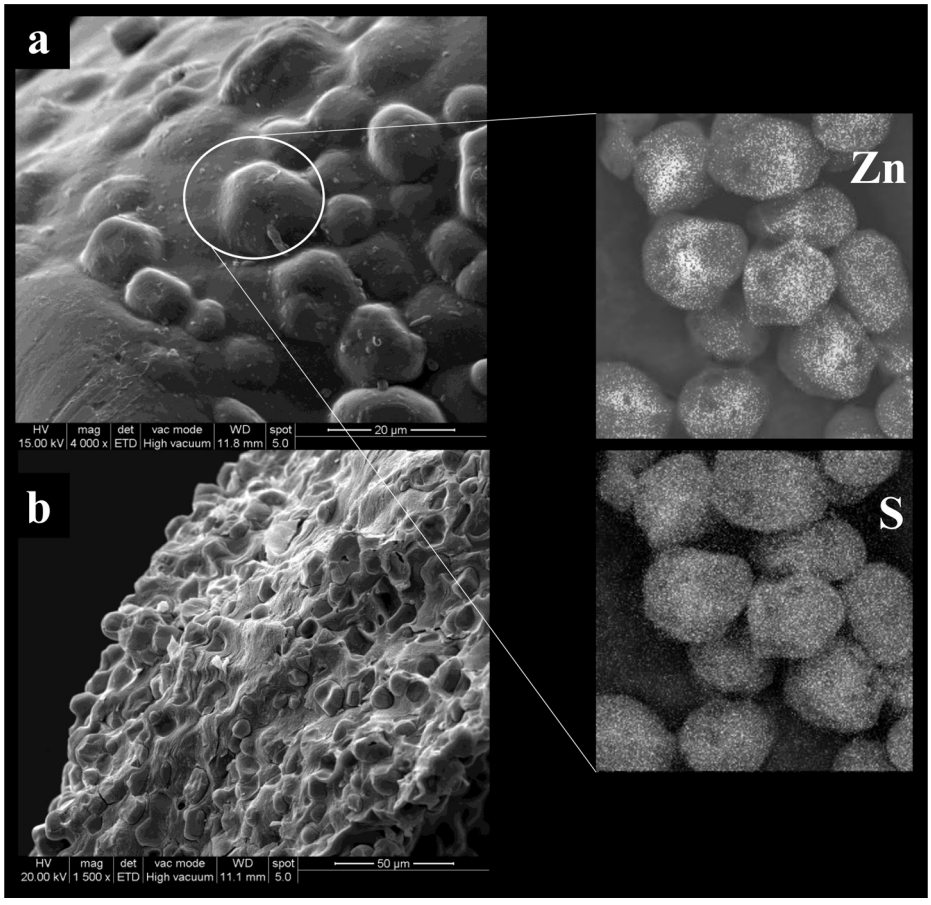

Fig. 3. SEM micrographs of (a) the surface and (b) cross-section of corn starch-calcium alginate beads with yerba mate extract and zinc (Zn) and sulfur (S) surface mapping on native starch granules loaded with zinc sulfate obtained by SEM-EDX (magnification 2000×).

preformed calcium cross-linked beads and subsequently loading them with iron. In this work, the selection of the adequate concentration of zinc into the starch-carrier constituted a successful strategy to avoid the production of deformed beads or beads with tail.

3.2.3. Loading capacity and antioxidant activity of the beads

Starch-alginate beads with zinc and yerba mate polyphenols were obtained (ZY-beads). The zinc concentration in ZY-beads was much higher than in control beads; values around 9.2 mg Zn^{2+}/g dried beads were obtained for ZY-beads while control ones showed values around 0.09 mg Zn^{2+}/g dried beads. The negligible zinc amount in the control sample could be attributed to the concentration present in the raw yerba mate extract (around 2 mg Zn^{2+}/L extract). With respect to the polyphenols content, no statistically significant differences were found between ZY-beads and control beads obtaining values of around 32 mg of yerba mate polyphenols/g dried beads for both samples.

The antioxidant activity was assessed using the DPPH radical scavenging method and β-carotene-linoleic acid model system (Table 1). Control and ZY-beads showed a strong inhibitory activity towards DPPH radical. Both types of beads showed no statistically significant differences, which indicated that the zinc presence did not modify the antioxidant activity of the yerba mate extract. Previously, we have observed that the gelation and drying stages did not modify the antioxidant activity of this extract, regardless of the addition of starch into the alginate matrix (López Córdoba et al., 2013, 2014).

For the antioxidant activity determined by the β-carotene bleaching method, no statistically significant differences were found between the samples (Table 1). Few literature data was found dealing with the antioxidant activity of encapsulated Zn. Nevertheless, Zn^{2+} has been shown to have an antioxidant role in defined chemical systems: zinc can protect membranes from transition metal-initiated lipid oxidation by occupying negatively charged sites with potential metal binding capacity (Zago & Oteiza, 2001).

3.2.4. FTIR and DSC analysis

Fig. 5 shows IR spectra of native corn starch, starch-zinc carriers and zinc sulfate. Similar spectra were obtained for the starches-zinc carrier and the native corn starch; signals around 1156, 1080 and 1019 cm^{-1} were attributed to vibrations of C—O and C—C groups of starch polymer. The band located around 3390 cm^{-1} corresponds to the stretching of —OH groups (Błaszczak, Valverde, & Fornal, 2005; Kizil, Irudayaraj, & Seetharaman, 2002). Besides, the spectra of the starch-zinc carriers (S-ZnL and S-ZnH) showed signals at 1115 and 624 cm^{-1}, also observed in the zinc sulfate spectrum, corresponding to the vibrations modes of the SO_4^{-2} groups (Wang, Du, & Liu, 2004). The adsorption of transition metal salts on the native and modified starches have been already investigated. For example, Ciesielski, Lii, Yen, and Tomasik (2003) and Tomasik, Anderegg, Baczkowicz, and Jane (2001) found that starch-metal complexes are formed because the anion penetrates into the starch granules, and the cation is held by electrostatic attractions.

IR spectra of sodium alginate, control and ZY-beads are shown in Fig. 6. For the sodium alginate (SA), characteristic functional groups

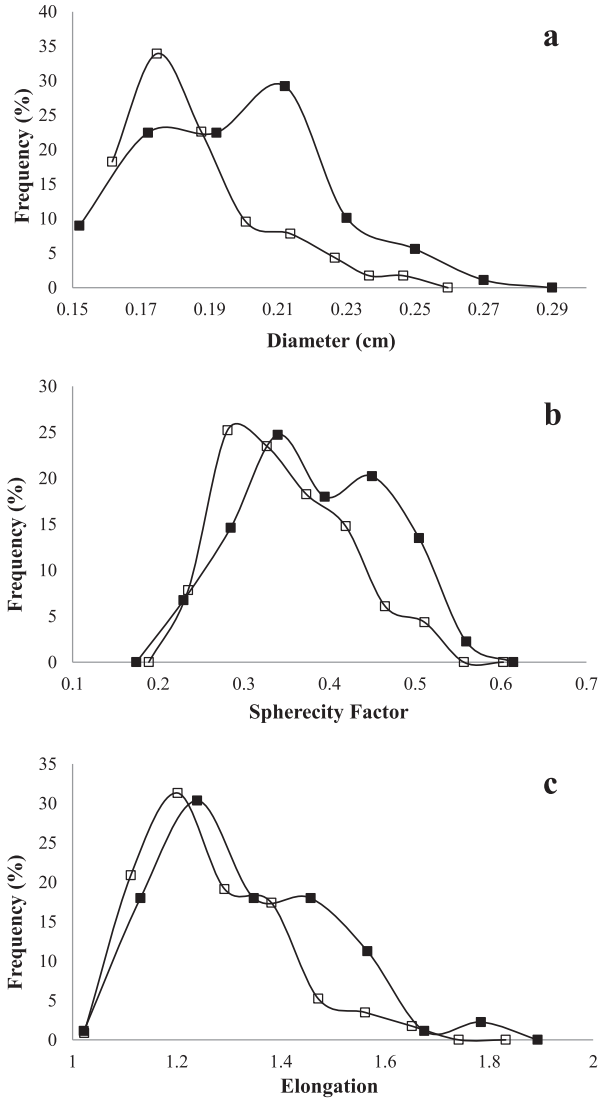

Fig. 4. Distributions of (a) diameter, (b) sphericity and (c) elongation for control (■) and ZY (▫) beads.

(COO− stretching) were present, with a broad asymmetrical band at 1610 cm^{-1} and a narrower symmetrical band at 1415 cm^{-1}. Control (C-beads) and ZY-beads showed characteristic signals of the functional groups of alginate and corn starch polymers. However, a shift in the carbonyl stretching vibrations from 1610 to 1634 cm^{-1} was observed for both types of beads. According to Taha, Nasser, Ardakani, and AlKhatib (2008) this effect could be due to the stronger ionic nature of the carboxylate–calcium interaction, which allow more free delocalization of the carboxylate electrons and reduce the double-bond character of the carboxylic carbonyls.

Table 1
DPPH• radical scavenging activity and inhibitory activity of the β-carotene bleaching for control and ZY-beads.

Sample	DPPH• radical inhibition (%)	β-carotene bleaching Inhibition (%)
Control beads	$83.3^{a} \pm 4.4$	$69.4^{b} \pm 0.7$
ZY-beads	$81.5^{a} \pm 4.2$	$75.9^{b} \pm 1.1$

Same superscript indicate no statistically significant differences ($\alpha = 0.05$).

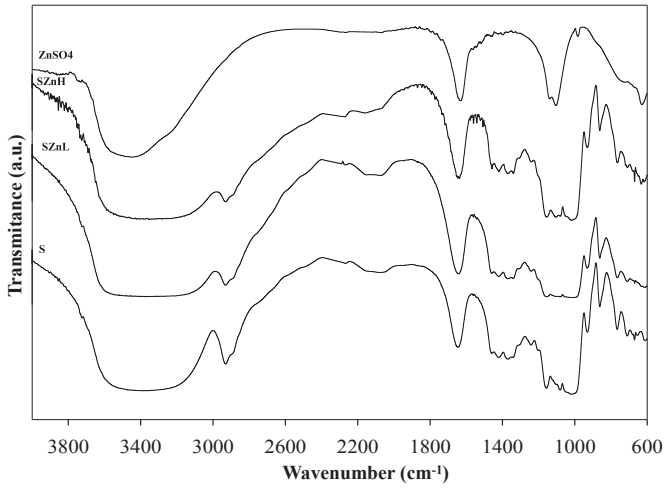

Fig. 5. IR spectra of native corn starch (S), starch-zinc carriers (S-ZnL and S-ZnH) and zinc sulfate.

Moreover, in the ZY-beads (Fig. 6) no new signals were observed as compared to control ones and the vibration frequency of the COO- groups was not modified. Several authors reported that this band is found around 1643 cm^{-1} in zinc-crosslinked alginate beads, which is probably related to the formation of coordinate bonds between the carboxylate moieties of alginic acid and zinc ions, increasing the double bond character of carboxylic carbonyls (Chan et al., 2002; Taha et al., 2008). Thus, these facts would indicate that not chemical interaction between zinc and the encapsulating matrix was detected in the present work.

The DSC thermal analysis for sodium alginate, control and ZY-beads was carried out (Fig. 7). Sodium alginate showed an exothermic peak at 225 °C as a result of the breakdown of the polymer (Mimmo, Marzadori, Montecchio, & Gessa, 2005).

Both types of beads showed an endothermic peak around 195 °C; however, this peak was broader for ZY-beads than for control ones. Besides, the characteristic decomposition peak of sodium alginate exhibited a shift from 225 to 250 °C due to the formation of the structure of "egg box" with calcium ions (Fernández-Hervás, Holgado, Fini, & Fell, 1998). Taha et al. (2008) assessed the production of alginate beads with zinc as cross-linking agent and found that the matrix exhibited an exothermic peak at around 200 °C. This peak was also present in the thermal profile of sodium alginate, albeit at higher temperatures (*ca.*

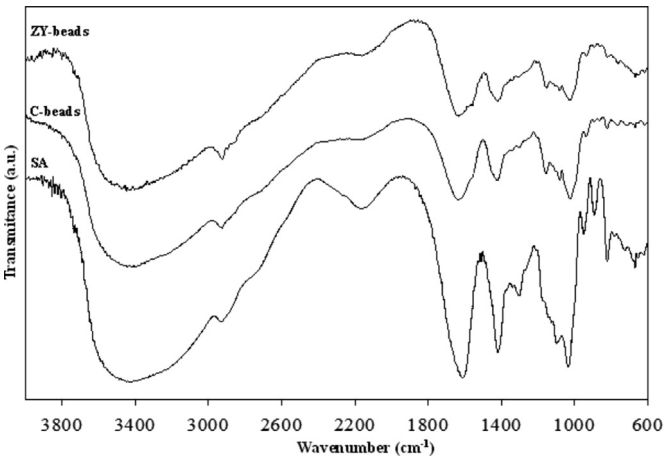

Fig. 6. IR spectra of sodium alginate (SA), control beads (C-beads) and zinc-yerba mate beads (ZY-beads).

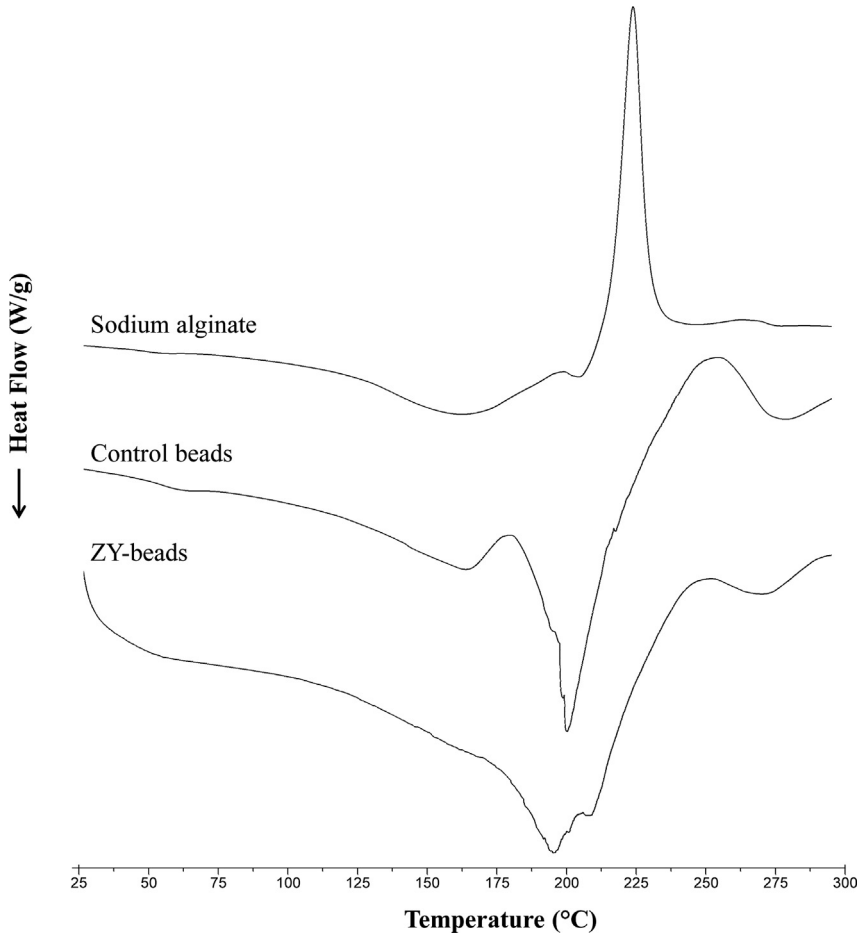

Fig. 7. DSC thermograms for sodium alginate, control beads and ZY-beads.

220 °C). These authors proposed that the shift to lower temperature is related to zinc-induced degradation of alginate. According to these findings in our work, no crosslinking between zinc and alginate would be taking place. If zinc alginate had formed, changes in the shape and the texture of the capsules would have been observed on a macroscopic scale. In fact, DSC and FT-IR analysis could not detect changes in the matrix associated with zinc presence. These results indicated that the proposed methodology, allowed obtaining a compartmentalized encapsulation system, where the active compounds coexists simultaneously without interfering.

4. Conclusion

The incorporation of a starch-zinc carrier into the calcium alginate beads with yerba mate extract, allowed obtaining a compartmentalized system without affecting their morphological characteristics. Moreover, the beads exhibited a strong inhibitory activity towards free radicals. The proposed methodology could be used for the simultaneous transport of other active compounds when a possible interaction should be avoided. The encapsulation systems obtained could be employed in the formulation of new antioxidants-rich foods with enhanced healthy properties.

Acknowledgments

The authors would like to thank the Instituto Nacional de la Yerba Mate (INYM) for their support through the PRASY project and to the Argentinean National Research Council (CONICET). In memory of Dr. Miriam Martino (1958–2014). Lead Scientist, CIDCA-CONICET, Argentina. A highly respected colleague, mentor and friend of many years, who will be greatly missed.

References

Belščak-Cvitanović, A., Stojanović, R., Manojlović, V., Komes, D., Cindrić, I. J., Nedović, V., et al. (2011). Encapsulation of polyphenolic antioxidants from medicinal plant extracts in alginate – chitosan system enhanced with ascorbic acid by electrostatic extrusion. *Food Research International, 44*(4), 1094–1101.

Błaszczak, W., Valverde, S., & Fornal, J. (2005). Effect of high pressure on the structure of potato starch. *Carbohydrate Polymers, 59*(3), 377–383.

Bracesco, N., Sanchez, A. G., Contreras, V., Menini, T., & Gugliucci, A. (2011). Recent advances on *Ilex paraguariensis* research: minireview. *Journal of Ethnopharmacology, 136*(3), 378–384.

Brand-Williams, W., Cuvelier, M. E., & Berset, C. (1995). Use of a free radical method to evaluate antioxidant activity. *Lebensmittel-Wissenschaft & Technologie, 28*(1), 25–30.

Brewer, M. S. (2011). Natural antioxidants: sources, compounds, mechanisms of action, and potential applications. *Comprehensive Reviews in Food Science and Food Safety, 10*(4), 221–247.

Chan, E.-S., Lee, B.-B., Ravindra, P., & Poncelet, D. (2009). Prediction models for shape and size of ca-alginate macrobeads produced through extrusion-dripping method. *Journal of Colloid and Interface Science, 338*(1), 63–72.

Chan, L. W., Jin, Y., & Heng, P. W. S. (2002). Cross-linking mechanisms of calcium and zinc in production of alginate microspheres. *International Journal of Pharmaceutics, 242*(1–2), 255–258.

Ciesielski, W., Lii, C.-y., Yen, M.-T., & Tomasik, P. (2003). Interactions of starch with salts of metals from the transition groups. *Carbohydrate Polymers, 51*(1), 47–56.

Day, L., Seymour, R. B., Pitts, K. F., Konczak, I., & Lundin, L. (2009). Incorporation of functional ingredients into foods. *Trends in Food Science & Technology, 20*(9), 388–395.

Deladino, L., Anbinder, P. S., Navarro, A. S., & Martino, M. N. (2008). Encapsulation of natural antioxidants extracted from *Ilex paraguariensis*. *Carbohydrate Polymers, 71*(1), 126–134.

Fernández-Hervás, M. J., Holgado, M. A., Fini, A., & Fell, J. T. (1998). In vitro evaluation of alginate beads of a diclofenac salt. *International Journal of Pharmaceutics, 163*(1–2), 23–34.

Fundueanu, G., Nastruzzi, C., Carpov, A., Desbrieres, J., & Rinaudo, M. (1999). Physico-chemical characterization of Ca-alginate microparticles produced with different methods. *Biomaterials, 20*(15), 1427–1435.

George, M., & Abraham, T. E. (2006). Polyionic hydrocolloids for the intestinal delivery of protein drugs: alginate and chitosan: a review. *Journal of Controlled Release, 114*(1), 1–14.

Goel, A., Dani, V., & Dhawan, D. K. (2005). Protective effects of zinc on lipid peroxidation, antioxidant enzymes and hepatic histoarchitecture in chlorpyrifos-induced toxicity. *Chemico-Biological Interactions, 156*(2–3), 131–140.

Heck, C. I., & González de Mejía, E. (2007). Yerba mate tea (*Ilex paraguariensis*): a comprehensive review on chemistry, health implications, and technological considerations. *Journal of Food Science, 72*(9), R138–R151.

Hercberg, S., Galan, P., Preziosi, P, Bertrais, S., Mennen, L., Malvy, D., et al. (2004). The su.vi.max study: a randomized, placebo-controlled trial of the health effects of antioxidant vitamins and minerals. *Archives of Internal Medicine, 164*(21), 2335–2342.

Kizil, R., Irudayaraj, J., & Seetharaman, K. (2002). Characterization of irradiated starches by using FT-Raman and FTIR spectroscopy. *Journal of Agricultural and Food Chemistry, 50*(14), 3912–3918.

Lesmes, U., & McClements, D. J. (2009). Structure–function relationships to guide rational design and fabrication of particulate food delivery systems. *Trends in Food Science & Technology, 20*(10), 448–457.

López Córdoba, A., Deladino, L., & Martino, M. (2013). Effect of starch filler on calcium-alginate hydrogels loaded with yerba mate antioxidants. *Carbohydrate Polymers, 95*(1), 315–323.

López Córdoba, A., Deladino, L., & Martino, M. (2014). Release of yerba mate antioxidants from corn starch–alginate capsules as affected by structure. *Carbohydrate Polymers, 99*(0), 150–157.

Luo, Z., Cheng, W., Chen, H., Fu, X., Peng, X., Luo, F., et al. (2013). Preparation and properties of enzyme-modified cassava starch-zinc complexes. *Journal of Agricultural and Food Chemistry, 61*(19), 4631–4638.

Mimmo, T., Marzadori, C., Montecchio, D., & Gessa, C. (2005). Characterisation of Ca– and Al–pectate gels by thermal analysis and FT-IR spectroscopy. *Carbohydrate Research, 340*(16), 2510–2519.

Perez-Moral, N., Gonzalez, M. C., & Parker, R. (2013). Preparation of iron-loaded alginate gel beads and their release characteristics under simulated gastrointestinal conditions. *Food Hydrocolloids, 31*(1), 114–120.

Prasad, A. S., Bao, B., Beck, F. W. J., Kucuk, O., & Sarkar, F. H. (2004). Antioxidant effect of zinc in humans. *Free Radical Biology and Medicine, 37*(8), 1182–1190.

Rassis, D. K., Saguy, I. S., & Nussinovitch, A. (2002). Collapse, shrinkage and structural changes in dried alginate gels containing fillers. *Food Hydrocolloids, 16*(2), 139–151.

Salgueiro, M. J., Zubillaga, M., Lysionek, A., Sarabia, M. I., Caro, R., De Paoli, T., et al. (2000). Zinc as an essential micronutrient: a review. *Nutrition Research, 20*(5), 737–755.

Schneider, C. A., Rasband, W. S., & Eliceiri, K. W. (2012). NIH Image to ImageJ: 25 years of image analysis. *Nature Methods, 9*(7), 671–675.

Singleton, V. L., Orthofer, R., & Lamuela-Raventós, R. M. (1999). *Analysis of total phenols and other oxidation substrates and antioxidants by means of folin-ciocalteu reagent*. In P. Lester (Ed.), *Methods in enzymology* (Vol. 299); (pp. 152–178). Academic Press.

Smigielska, H., & Thanh-Blicharz, J. L. (2010). Research on zinc fortified potato starch and on its use in dessert production. *Acta Scientiarum Polonorum Technologia Alimentaria, 9*(2), 217–226.

Taha, M. O., Nasser, W., Ardakani, A., & AlKhatib, H. S. (2008). Sodium lauryl sulfate impedes drug release from zinc-crosslinked alginate beads: switching from enteric coating release into biphasic profiles. *International Journal of Pharmaceutics, 350*(1–2), 291–300.

Tapiero, H., & Tew, K. D. (2003). Trace elements in human physiology and pathology: zinc and metallothioneins. *Biomedicine & Pharmacotherapy, 57*(9), 399–411.

Tomasik, P., Anderegg, J. W., Baczkowicz, M., & Jane, J. L. (2001). Potato starch derivatives with some chemically bound bioelements. *Acta Poloniae Pharmaceutica, 58*(6), 447–452.

Valerga, J., Reta, M., & Lanari, M. C. (2012). Polyphenol input to the antioxidant activity of yerba mate (*Ilex paraguariensis*) extracts. *LWT – Food Science and Technology, 45*(1), 28–35.

Wang, X., Du, Y., & Liu, H. (2004). Preparation, characterization and antimicrobial activity of chitosan–Zn complex. *Carbohydrate Polymers, 56*(1), 21–26.

WHO. (2002). *The world health report: Reducing risks, promoting healthy life*. http://www.who.int/whr/2002/en/whr02_en.pdf.

Yang, Y., Zhang, Z., Li, S., Ye, X., Li, X., & He, K. (2014). Synergy effects of herb extracts: Pharmacokinetics and pharmacodynamic basis. *Fitoterapia, 92*(0), 133–147.

Zago, M. P., & Oteiza, P. I. (2001). The antioxidant properties of zinc: interactions with iron and antioxidants. *Free Radical Biology and Medicine, 31*(2), 266–274.